Pergamon

Tetrahedron: *Asymmetry* 12 (2001) 1621–1624

TETRAHEDRON:
*ASYMMETRY*

# Conformational diastereoisomers of $PPh_3$ coordinated to stereogenic metal centres as molecular optical switches

Andrew P. Ayscough,[a] James F. Costello[b,]* and Stephen G. Davies[a,]*

[a] *Dyson Perrins Laboratory, University of Oxford, South Parks Road, Oxford OX1 3QY, UK*
[b] *Department of Chemistry, University of the West of England, Coldharbour Lane, Bristol BS16 1QY, UK*

Received 23 May 2001; accepted 29 May 2001

**Abstract**—The specific rotation of ($R_{Fe}$,*R*,*M*)-**4** *switches* sign upon epimerisation to ($R_{Fe}$,*S*,*P*)-**5**. X-Ray crystallographic studies suggest that inversion of the propeller configuration of the coordinated $PPh_3$ ligand is a major contributor to the switch of specific rotation. A simple model for predicting the conformational diastereoisomeric forms of $PPh_3$ is presented, suggesting future routes towards the design of molecular optical switching devices. © 2001 Elsevier Science Ltd. All rights reserved.

## 1. Introduction

Correlating the conformations of chiral molecules with macroscopic phenomena such as optical rotation[1] provides a rational basis for the design of molecular switching devices.[2] The explosion of interest in chiral optical switches[3] for molecular information storage systems has relied chiefly upon the reversible inversion of helical chirality.[4] Although the solid-state enantiomeric conformations (*M* and *P*) of metal coordinated $PPh_3$ **1** (Fig. 1) have been characterised many times,[5] to our knowledge the diastereoisomeric conformational control of such systems has yet to be addressed. We have previously rationalised the conformational preferences of molecular propellers in achiral,[6,7] prochiral[8] and stereogenic[9] complexes. We now report optical switching in chiral organometallic complexes of type **2**, which we postulate to derive from the chiral propeller conformations adopted by the coordinated $PPh_3$ ligand.

## 2. Results and discussion

The complex ($R_{Fe}$,*R*)-**4** may be prepared as previously reported in the racemic series via the diastereoselective reduction of the enantiomerically pure alkoxycarbene ($R_{Fe}$)-**3**† in 92% yield (Scheme 1).[10] Subsequent epimerisation of ($R_{Fe}$,*R*)-**4** with $SiO_2$ affords the thermodynamically preferred complex ($R_{Fe}$,*S*)-**5** in 98% yield. In common with enantiomerically pure complexes of *R* configuration at iron (irrespective of the stereochemistry, which may be present within the organic fragment $L^1$) the specific rotations of ($R_{Fe}$)-**3** $\{[\alpha]_D^{20}=-321$ (*c* 0.059, $CHCl_3$)} and ($R_{Fe}$,*S*)-**5** $\{[\alpha]_D^{20}=-320$ (*c* 0.042, $C_6H_6$)} are negative. Remarkably, the specific rotation of ($R_{Fe}$,*R*)-**4** $\{[\alpha]_D^{20}=+535$ (*c* 0.065, $C_6H_6$)} is not only *opposite* in sign to both ($R_{Fe}$)-**3** and ($R_{Fe}$,*S*)-**5**, but differs in magnitude by 855. Thus, epimerisation of ($R_{Fe}$,*R*)-**4**→($R_{Fe}$,*S*)-**5** is accompanied by a switch in the sign of specific rotation.

Solid-state studies by others and ourselves demonstrate that chiral complexes of the form $[M(\eta^5\text{-}C_5H_5)(PPh_3)(L^1)(L^2)]$ **2** exist as conformational diastereoisomers by virtue of the stereogenic propeller configurations (*P* or *M*) of the coordinated ligand $PPh_3$ **1** (Fig. 1).[11] For

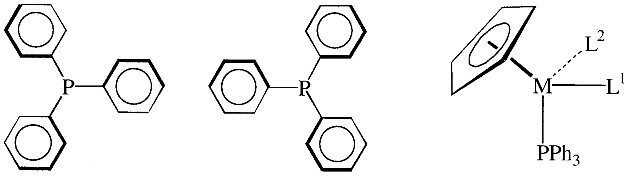

***P*-1** ***M*-1** **2**

**6** M = Fe
$L^1$ = -CHO
$L^2$ = -CO

**Figure 1.** Stereogenic propeller configurations *P*-**1** and *M*-**1**, the generic complex **2**, and **6**.

---

* Corresponding authors. E-mail: james.costello@uwe.ac.uk; steve.davies@chem.ox.ac.uk

† Experiments were conducted upon the $S_{Fe}$ series, but for clarity of exposition we discuss the degenerate $R_{Fe}$ series here.

0957-4166/01/$ - see front matter © 2001 Elsevier Science Ltd. All rights reserved.
PII: S0957-4166(01)00253-1

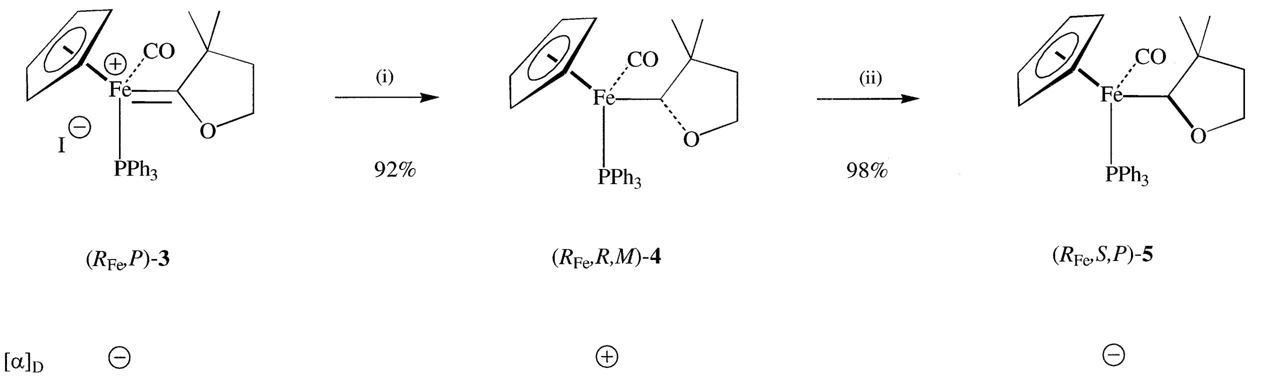

**Scheme 1.** *Reagents and conditions*: (i) $NaBH_4$, THF, −78°C; (ii) $SiO_2$, $Et_2O$.

example, the predominant conformational diastereoisomer observed in the series M = Fe and $L^2$ = CO is ($R_{Fe}S_{Fe}$,$PM$), e.g. **3** and **5** (Scheme 1). The X-ray crystal structure of ($R_{Fe}$,$S$,$P$)-**5** (viewed along $C_\alpha$–Fe bond axis, Fig. 2b) is consistent with this observation.[12]

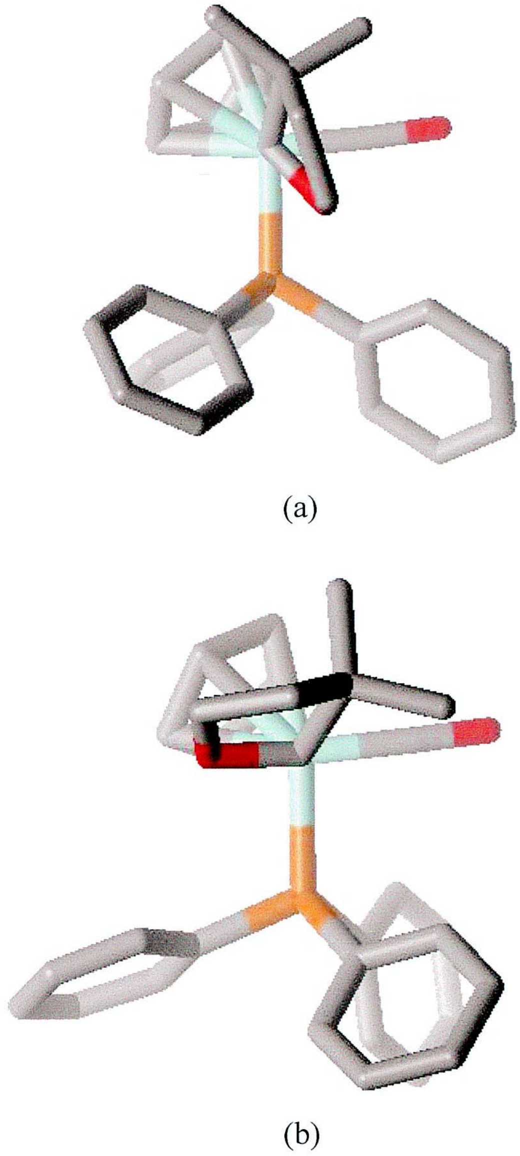

**Figure 2.** The X-ray crystal structures of: (a) ($R_{Fe}$,$R$,$M$)-**4** and (b) ($R_{Fe}$,$S$,$P$)-**5a** (viewed along Fe→P).

However, the corresponding view of the X-ray crystal structure of ($R_{Fe}$,$R$,$M$)-**4** (Fig. 2a) demonstrates the presence of a conformational diastereoisomer of opposite propeller configuration. The difference in optical properties therefore provides compelling evidence for a connection between the conformational diastereoisomers ($R_{Fe}$,$R$,$M$)-**4** and ($R_{Fe}$,$S$,$P$)-**5** in the solid state and in solution. Furthermore, this is consistent with the $PPh_3$ rotor configuration being the major contributor to the change in sign of the specific rotation.

A series of calculations supported by extensive X-ray crystal structure correlations serve to establish the origin of this conformational anomaly with a view to understanding and ultimately controlling the diastereoisomeric conformations of ($PM$)-**1**. Complexes such as **2** adopt a pseudo-octahedral geometry where the monodentate ligands ($PPh_3$, $L^1$ and $L^2$) are essentially orthogonal to each other, occupying adjacent sites of an octahedron. The $\eta^5$-$C_5H_5$ ligand occupies the three remaining coordination sites. A Newman projection (viewed along $L^1$–M) of ($R$)-**6** (**2**, where $L^1$ = -CHO and $L^2$ = CO, Fig. 3a) demonstrates the three quadrants[13] **A**–**C** available for occupation by $L^1$. Quadrant **A** is the least sterically demanding site for occupation by atoms or groups associated with $L^1$. Quadrants **B**→**C** are progressively less accessible to $L^1$.[13] Penetration of atoms or groups associated with $L^1$ below the plane defined by $L^1$–M–$L^2$ into quadrants **B**/**C** clearly affect the conformational preferences of the $PPh_3$ ligand. Calculations[‡] were performed to characterise the preferred conformational diastereoisomeric arrangements of $PPh_3$ in ($R$)-**6** as the oxygen atom of $L^1$ is driven through quadrants **A**→**B**→**C**. The torsion angle P–Fe–C(H)=O ($\Phi$) was driven through the range 0→360° in 15° increments. At each point, the $PPh_3$ fragment in ($R$)-**6** was subjected to a full conformational analysis. The initial symmetry of $PPh_3$ for each set of calculations was $C_{3v}$ [i.e. $C_o$–$\mathbf{C}_i$–**P**–M ($\omega$) for all three rings = 0°]. A phenyl ring of the $PPh_3$ fragment was placed between the $\eta^5$-$C_5H_5$ and CO ligands (via P–M bond rotation) and then driven through the range $\omega_1 = 0 \rightarrow 180°$ in 10° increments. At each increment, the two remaining rings were also driven independently

---

[‡] Calculations[7] were conducted using the Chem-X package (1999.2) supported on the Windows NT platform using a Pentium personal computer. Chem-X is distributed by Chemical Design Ltd., Oxford Molecular Group, The Medawar Centre, Oxford Science Park, Oxford OX4 4GA, UK.

($\omega = 0 \rightarrow 180°$ in 20° increments) with concomitant minimisation about all rotatable bonds [P–C, M–P and M–($\eta^5$-$C_5H_5$)$_{cent}$] until the default energy convergence criteria was achieved. A plot of the thermodynamically preferred epimeric conformations [i.e. ($R_{Fe}$,*P*) (■) or ($R_{Fe}$,*M*) (□)] of the $PPh_3$ fragment within (*R*)-**6** as *Φ* varies is presented in Fig. 4; identical arguments apply to the degenerate case of ($S_{Fe}$,*M*) (■) and ($S_{Fe}$,*P*) (□), respectively.

The thermodynamically preferred conformation of (*R*)-**6** [and thus (*S*)-**6**] orients the formyl C(H)=O group approximately *anti* to the M–CO bond ($\Phi$ = ca. −60°). This arrangement is accompanied by the *P* (■) propeller configuration of the $PPh_3$ fragment, i.e. ($R_{Fe}$,*P*). The *anti* ($\Phi$ = ca. −60°) epimeric conformational diastereoisomer ($R_{Fe}$,*M*)-**6**, possessing an inverted propeller configuration, is calculated to be 8 kJ/mol higher in energy. The *syn* conformer ($\Phi$ = ca. +135°), which

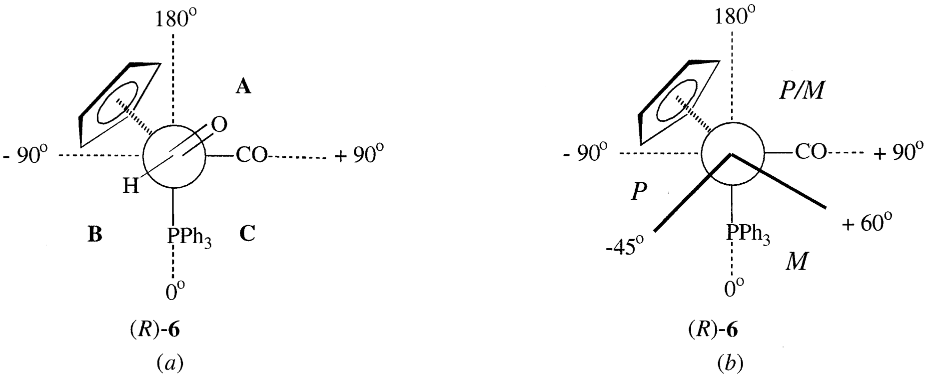

**Figure 3.** Newman projections of (*R*)-**6** ($C_\alpha \rightarrow Fe$) illustrating: (a) quadrants **A**–**C** and (b) zones of propeller preferences (monodentate ligands excluded for clarity). In the case of (*S*)-**6**, the propeller preferences are reversed.

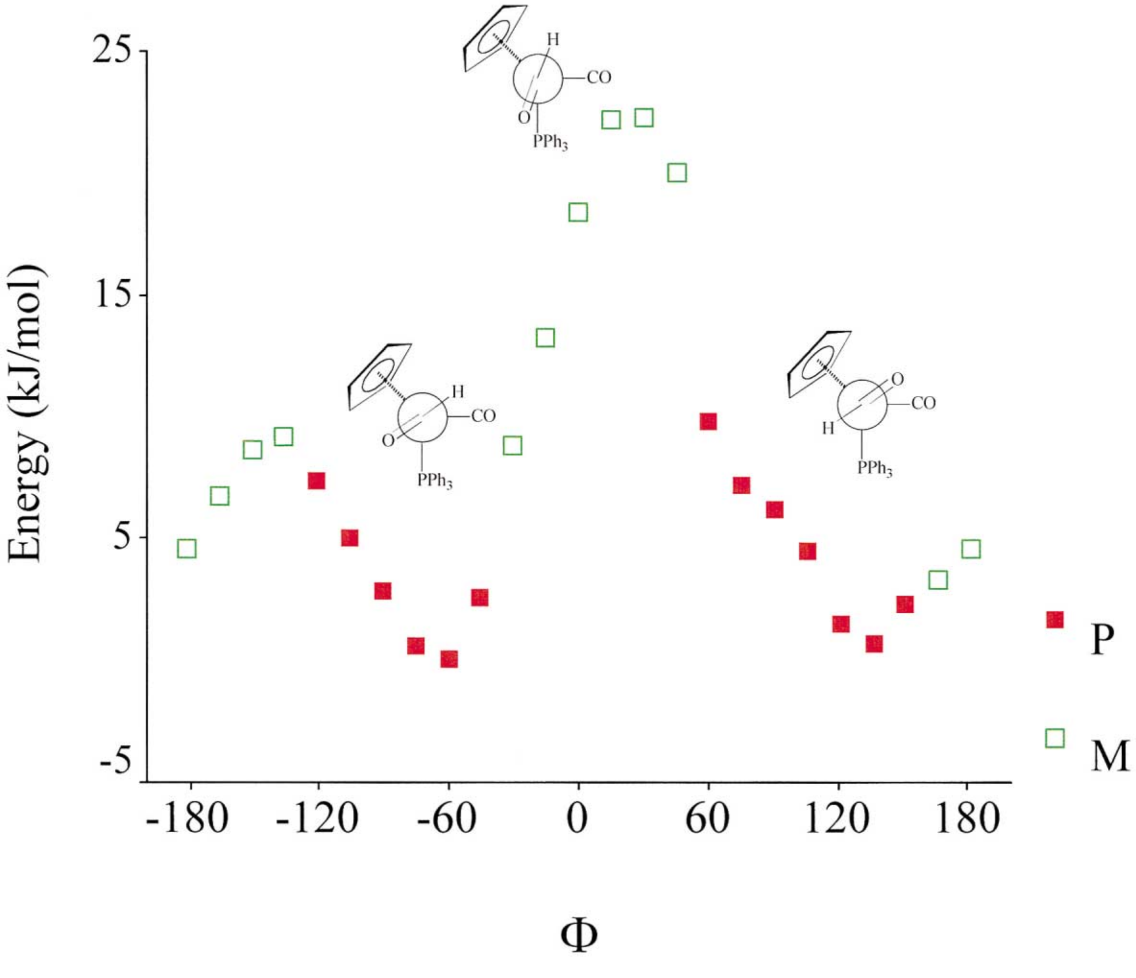

**Figure 4.** The thermodynamically preferred conformations of the $PPh_3$ fragment [($R_{Fe}$,*P*) (■) and ($R_{Fe}$,*M*) (□)] in (*R*)-**6** as P–Fe–C(H)=O (*Φ*) is driven $0 \rightarrow \pm 180°$.

also prefers the ($R_{\text{Fe}}$,$P$) arrangement, is similar in energy to the global minimum ($\Delta E = 0.5$ kJ/mol). Fig. 4 demonstrates, however, that the rotation of the formyl group from *anti* ($\Phi$ = ca. −60°) to *syn* ($\Phi$ = ca. +135°) is accompanied by an inversion of the stereogenic sense of the propeller configuration of the $PPh_3$ ligand, at $\Phi \approx -130, -45, +60$ and +150°. The relationship between the orientation of the oxygen atom associated with the formyl ligand ($\Phi$) and the preferred conformational diastereoisomeric forms of (*R*)-**6** are summarised in Fig. 3b. The *P* propeller configuration is clearly favoured as the oxygen atom of the formyl group penetrates quadrant **B** ($\Phi = -90 \rightarrow -45°$). The overall energy of the system increases to a maximum as the oxygen atom passes through quadrants **B**→**C** ($\Phi = -45 \rightarrow 0 \rightarrow +60°$), eclipsing the M–P bond en route. Throughout this range ($R_{\text{Fe}}$,$M$)-**6** is favoured over ($R_{\text{Fe}}$,$P$)-**6** by up to 25 kJ/mol. As the oxygen atom approaches quadrant **A** ($\Phi = +60 \rightarrow +90 \rightarrow 180°$), the energy difference between ($R_{\text{Fe}}$,$P$)-**6** and ($R_{\text{Fe}}$,$M$)-**6** is calculated to be small, leading one to expect a mixture of both diastereoisomeric conformations.

All available crystallographic data[§] associated with complexes of type **2** (M = Fe, Re, Cr and Ru; $L^1 = \eta^1$-ligand and $L^2$ = CO or NO) are consistent with this model. In general, atoms or groups associated with $L^1$ dictate which conformational diastereoisomer is observed in the solid state. Conformational locking, resulting in the penetration of a sterically demanding atom or group (i.e. >H or $\sigma_{\text{nb}}$) into quadrants **B**/**C** ($\Phi = -45 \rightarrow 0 \rightarrow +60°$, Fig. 2b), confers the ($R_M S_M$,$MP$) conformational diastereoisomer. The alternative and more commonly encountered ($R_M S_M$,$PM$) arrangement is favoured when the penetrating atoms/groups lie in the range $\Phi = -45 \rightarrow \approx -90°$. When penetrating atoms/groups lie in the range $\Phi = +180 \rightarrow \approx +60°$, there can be no interference with the $PPh_3$ ligand and therefore mixtures of conformational diastereoisomers are observed.

As predicted by the model and as observed in the solid state for **4** [$\Phi = +44°$, for ($R_{\text{Fe}}$,$R$,$M$)], penetration of the oxygen substituent into quadrant **C** confers a preference for the ($R_{\text{Fe}}$,$R$,$M$) epimer (Scheme 1). Epimerisation of **4** reorients the oxygen substituent away from zone **C** [$\Phi = -90°$, for ($R_{\text{Fe}}$,$S$,$P$)], thereby favouring the alternative conformational diastereoisomer ($R_{\text{Fe}}$,$S$,$P$)-**5**.

## 3. Conclusion

In conclusion, for the $R_{\text{Fe}}$ complexes, the propeller configuration of $PPh_3$ *switches* from (*M*)-**4**→(*P*)-**5** on epimerisation at the α centre with a concomitant change in specific rotation from +535 to −320. Complexes designed to undergo controllable reversible optical switching using the above conformational analysis are currently being investigated.

## Acknowledgements

The authors would like to thank the Royal Society of Chemistry and the Leverhulme Trust for their support (J.F.C.).

## References

1. Kondru, R. K.; Wipf, P.; Beratan, D. N. *J. Phys. Chem. A* **1999**, *103*, 6603.
2. Kondru, R. K.; Wipf, P.; Beratan, D. N. *Science* **1998**, *282*, 2247.
3. Feringa, B. L.; van Delden, R. A.; Koumura, N.; Geertsema, E. M. *Chem. Rev.* **2000**, *100*, 1789.
4. (a) Zahn, S.; Canary, J. W. *Science* **2000**, *288*, 1404; (b) Huck, N. P. M.; Jager, W. F.; de Lange, B.; Feringa, B. L. *Science* **1996**, *273*, 1686; (c) Koumura, N.; Zijlstra, R. W. J.; van Delden, R. A.; Harada, N.; Feringa, B. L. *Nature* **1999**, *401*, 152.
5. For a recent example, see: Dance, I.; Scudder, M. *J. Chem. Soc., Dalton Trans. 1* **2000**, 1579.
6. Costello, J. F.; Davies, S. G. *J. Chem. Soc., Perkin Trans. 2* **1998**, 1683.
7. Barucki, H.; Coles, S. J.; Costello, J. F.; Gelbrich, T.; Hursthouse, M. B. *J. Chem. Soc., Dalton Trans. 1* **2000**, 2319.
8. Costello, J. F.; Davies, S. G.; McNally, D. *J. Chem. Soc., Perkin Trans. 2* **1999**, 465.
9. Barucki, H.; Coles, S. J.; Costello, J. F.; Hursthouse, M. B. *J. Organomet. Chem.* **2001**, *622*, 265.
10. Ayscough, A. P.; Davies, S. G. *J. Chem. Soc., Chem. Commun.* **1986**, 1648.
11. For example, see: Garner, S. E.; Orpen, A. G. *J. Chem. Soc., Dalton Trans. 1* **1993**, 533.
12. Davies, S. G.; Blackburn, B. K.; Whittaker, M. In *Stereochemistry of Organometallic and Inorganic Compounds*; Bernal, I., Ed.; Elsevier: Amsterdam, 1989; Vol. 3, p. 141.
13. Blackburn, B. K.; Davies, S. G.; Sutton, K. H.; Whittaker, M. *Chem. Soc. Rev.* **1988**, *17*, 147.

---

[§] Crystal structures were located within the October 1999 release of the Cambridge Structural Database (207,507 entries) using the QUEST program. Fletcher, D. A.; McMeeking, R. F.; Parkin, D. *J. Chem. Inf. Comput. Sci.* **1996**, *36*, 746. Supplementary data supplied.